Assignment-7
Experimental methods in Catalysis Assignment

Submitted by
Kundan Kumar (CA19M005)
Catalysis Technology

The effect of the internal magnetism of ferromagnetic catalysts on their catalytic activity toward oxygen reduction reaction

Introduction

Magnetic field effects can provide a handle on steering chemical reactions and manipulating yields. The presence of a magnetic field can influence the energy levels of the active species by interacting with their spin states. Here we demonstrate the effect of a magnetic field on the electrocatalytic processes taking place on platinum-based nanoparticles in fuel cell conditions.

In the oxygen reduction reaction (ORR), the oxygen transport rate plays an important role in the ORR on the cathode. An approach by applying magnetic fields on the cathode can effectively improve the oxygen transport. However, no work reports the effect of the magnetism of ferromagnetic catalysts on ORR under an external magnetic field.

The sluggish heterogeneous catalysis-oxygen reduction reaction is the main challenge for practical applications in fuel cells and metal-air batteries . The efficiency of ORR depends on not only the catalytic activity of cathode catalysts but also the oxygen transport rate that is affected by the presence of water. Among various cathode catalysts, Pt-based materials are known as the most promising ORR electrocatalysts, but their large-scale application was constrained by their scarcity, prohibitive cost, and limited durability of noble metals.

Therefore, a concerted effort has been devoted to develop low-cost ORR catalysts with competitive activity and durability, such as transition metal oxides, Fe3O4 , MnO2 , and metal-free carbon catalysts. In addition, the internal tiny magnetic fields of ferromagnetic atalysts can also be applied to fuel cells to affect the discharge performance on the cathode. at a low Fe3O4/polyaniline load density on the cathode electrode in a zinc air fuel cell, the tiny magnetic field can promote oxygen transfer, increase the electric double-layer capacitance, lower the charge transfer resistance, and improve the discharge performance. But, when the load density is higher than 7.11 mg cm−2, the internal tiny magnetic fields inhibit oxygen transfer because of the interactions between the different magnetic poles.

Electrochemical characterization

The electrochemical measurements were performed using an electrochemical workstation (CHI650). A common threeelectrode electrochemical cell was used for measurements. The counter and reference electrodes used were a platinum wire and an Ag/AgCl (saturated KCl solution) electrode, respectively.

The working electrode was a glassy carbon disk (5 mm in diameter). The thin-film electrode was prepared as follows: 2 mg of catalyst and 1 mg of XC-72 vulcan carbon (to improve the conductivity of the catalyst film) were dispersed ultrasonically in 0.4 mL Nafion/ethanol (0.25 % Nafion) solution, and 8 μL of the above solution was pipetted on the glassy carbon surface and dried at room temperature.

All currents were normalized by the geometric area of the electrode (0.196 cm2). All potentials initially measured versus the Ag/AgCl electrode were converted to the reversible hydrogen electrode (RHE). The prepared three-electrode system was settled in a magnetic field produced by a direct-current solenoid. The magnetic strength of 0.19, 0.37, or 0.56 T can be applied to the three-electrode system according to the following equation.

$$B = \mu_0 I\left(n/L\right)$$

where B is the magnetic strength, μ0 is the vacuum permeability, I is the current intensity, and n/L is the number of turns per length. The magnetic field is generated by a solenoid coil. In order to keep the temperature at 25 °C, the three-electrode cellwas wrapped by a water pipe, and water at a temperature of 25 °C flows through it during the experiment.

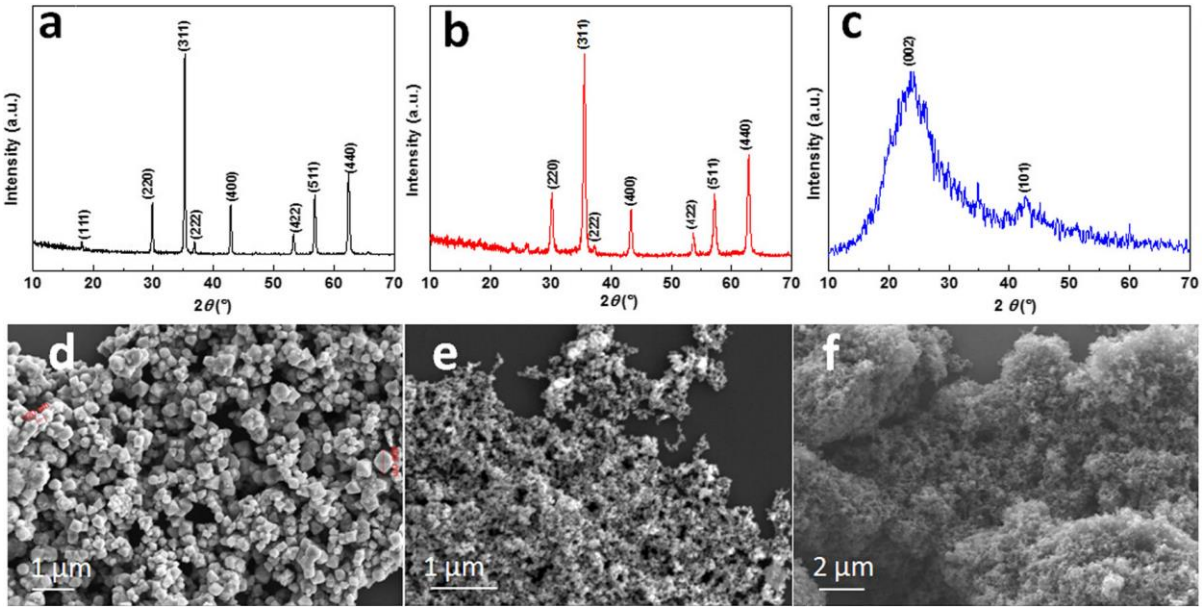

Fig-1 XRD patterns of Fe_3O_4 (a), γ-Fe_2O_3 (b), and Fe-N-C (c); SEM images of Fe_3O_4 (d), γ-Fe_2O_3 (e), and Fe-N-C (f)

Results:

The crystal structures of the purchased Fe3O4, γ-Fe2O3, and as-prepared Fe-N-C samples were characterized by XRD. As shown in Fig. 1a, the diffraction pattern of the planes (111), (220), (311), (222), (400), (422), (511), and (440) at 2θ values of 18.1°, 29.9°, 35.3°, 37.0°, 42.9°, 53.3°, 56.8°, and 62.4°, respectively, proves the presence of Fe3O4 .

Its average crystallite size calculated through the Scherrer formula of the (311) plane is about 250 nm. In the case of γ-Fe2O3 (Fig. 1b), the peaks at 18.1°, 30.2°, 35.6°, 37.2°, 43.2°, 53.6°, 57.3°, and 62.9° are the typical diffraction pattern of γ-Fe2O3 . The estimated crystallite size of γ-Fe2O3 is 20 nm. The Fe-N-C sample in Fig. 1c exhibits two peaks at about 24.4° and 42.8°, which could be ascribed to the (002) and (101) plane of the graphitic structure SEMimages of Fe3O4, γ-Fe2O3, and Fe-N-C are present in Fig. (1d-f). As seen in Fig. 1d, Fe3O4 mostly consists of

octahedral particles, and there is also a small amount of irregular polyhedron particles in the SEM image.
Its size ranges from 150 to 400 nm. The SEM image in Fig. 1e reveals γ-Fe2O3 particles have a sphere-like morphology, and the size of the spheres is ca. 20 nm. The Fe-N-C sample displays clusters of carbon spheres, which is similar to our previous report.

Magnetic hysteresis (M-H) loops of the three samples were measured at room temperature, and the data are presented in Fig. 2. three samples have ferromagnetic property at room temperature. The value of saturation magnetization (Ms) is 86.3, 68.5, and 0.78 emu g−1 for Fe3O4, γ-Fe2O3, and Fe-N-C, respectively.

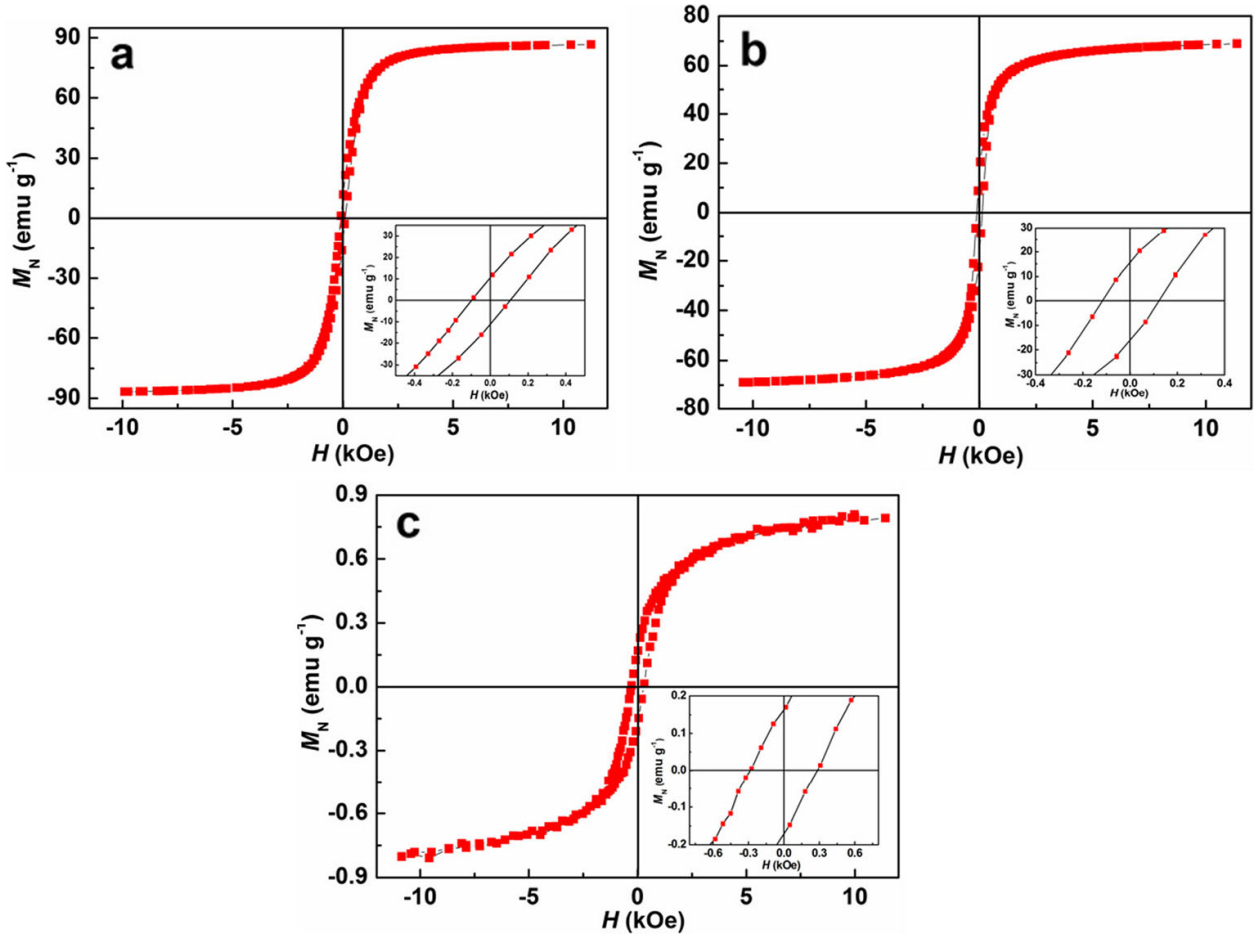

Fig. 2 Magnetic hysteresis loops of Fe3O4 (a), γ-Fe2O3 (b), and Fe-N-C (c). The corresponding inset shows a magnification of the hysteresis loop near zero fields

Figure 3 shows the cyclic voltammograms (CVs) of Fe3O4 (a), γ- Fe2O3 (b), and Fe-N-C electrodes, which were measured in a N2- or O2-saturated 0.1 mol L−1 KOH solution at a scan rate of 50 mV s−1 with and without the external magnetic field. For the all three catalysts, CVs in the potential range from −1.0 to +0.2 Vexhibited similar featureless curves. With the presence of N2 atmosphere, no obvious redox peaks. appear on the Fe3O4/C and Fe-N-C electrode (curves a, c), while redox peaks from −0.035 V to ca. +0.4 V were found on the γ-Fe2O3/C electrode, which could be related to the Fe(III)/Fe(II) redox system . In addition, the capacitive currents of the γ-Fe2O3/C and Fe-N-C electrodes are much higher than that of the Fe3O4/C electrode, since there is no non-porous structure in Fe3O4.

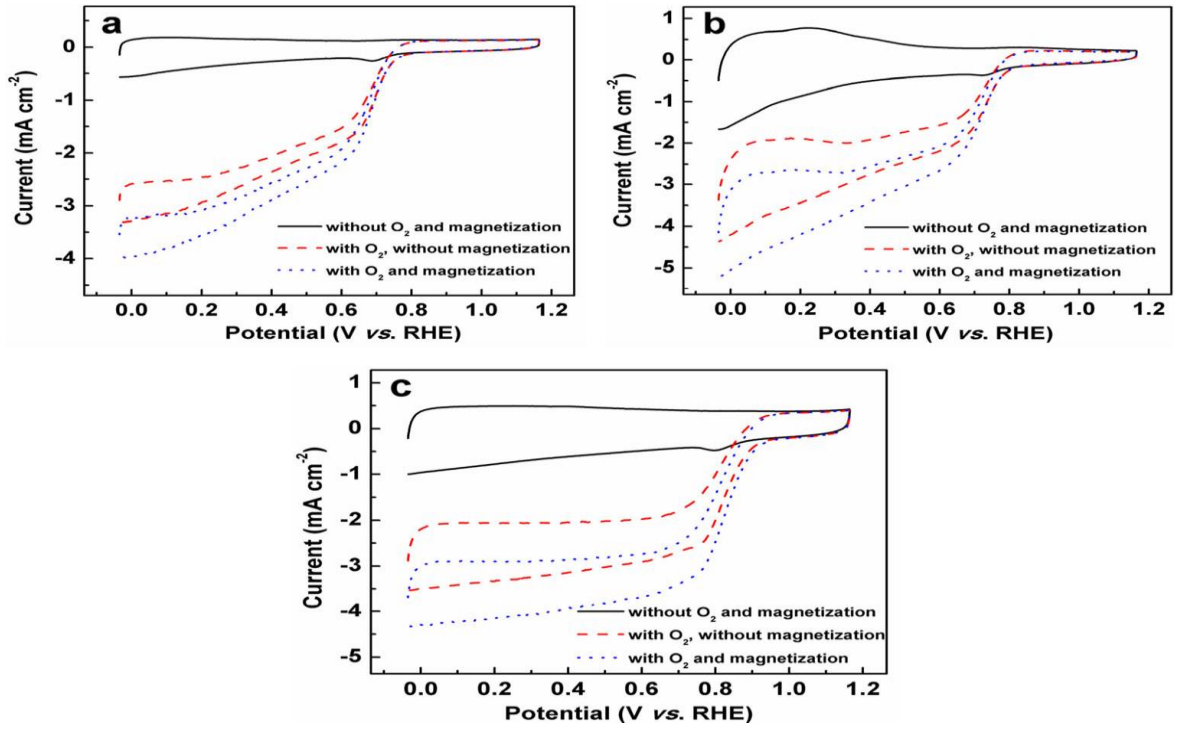

Fig-3 Cyclic voltammograms of Fe3O4/C (a), γ-Fe2O3/C (b), and Fe-N-C (c) at a potential scan rate of 50 mV s−1; electrolyte: 0.1 mol L−1 KOH; black solid lines the electrolyte saturated with N2 and without the presence of the external magnetic field; red dashed lines the electrolyte saturated with O2 and without the presence of the external magnetic field; blue dotted lines the electrolyte saturated with O2 and with the presence of the external magnetic field; magnetic field B = 0.56 T

Figure 4 shows LSVs of Fe3O4, γ-Fe2O3, and Fe-N-C(c) in O2-saturated 0.1 mol L−1 KOH electrolyte at a scan rate of 5mV s−1 with a rotation rate of 1600 rpm, and the corresponding increased ORR current at −0.4 V (vs. Ag/AgCl) for Fe3O4 (d), γ-Fe2O3 (e), and Fe-N-C (f) under different external magnetic fields. It shows that the ORR currents of the three catalysts increase with the strength of the external magnetic field. The high external magnetic field leads to the strong Kelvin (magnetic) force, which can facilitate the transfer of oxygen molecular, resulting in the higher ORR current. Meanwhile, the increased values of the ORR current are different among the three catalysts, which is similar to the results of CVs. The currents vs. strength of the external magnetic field was plotted in histograms shown in Fig. 4. It can be seen that the increased value of the ORR current under the same external magnetic field is different with each other on these three catalysts. For example, in the case of Fe3O4, the ORR current at 0.19 T increased by 1.6 %, while it is 2.5 and 7.7 % for γ-Fe2O3 and Fe-N-C, respectively. After comparing these values, the increased ORR currents of these three catalysts follow the order: Fe3O4 < γ-Fe2O3 < Fe-N-C.

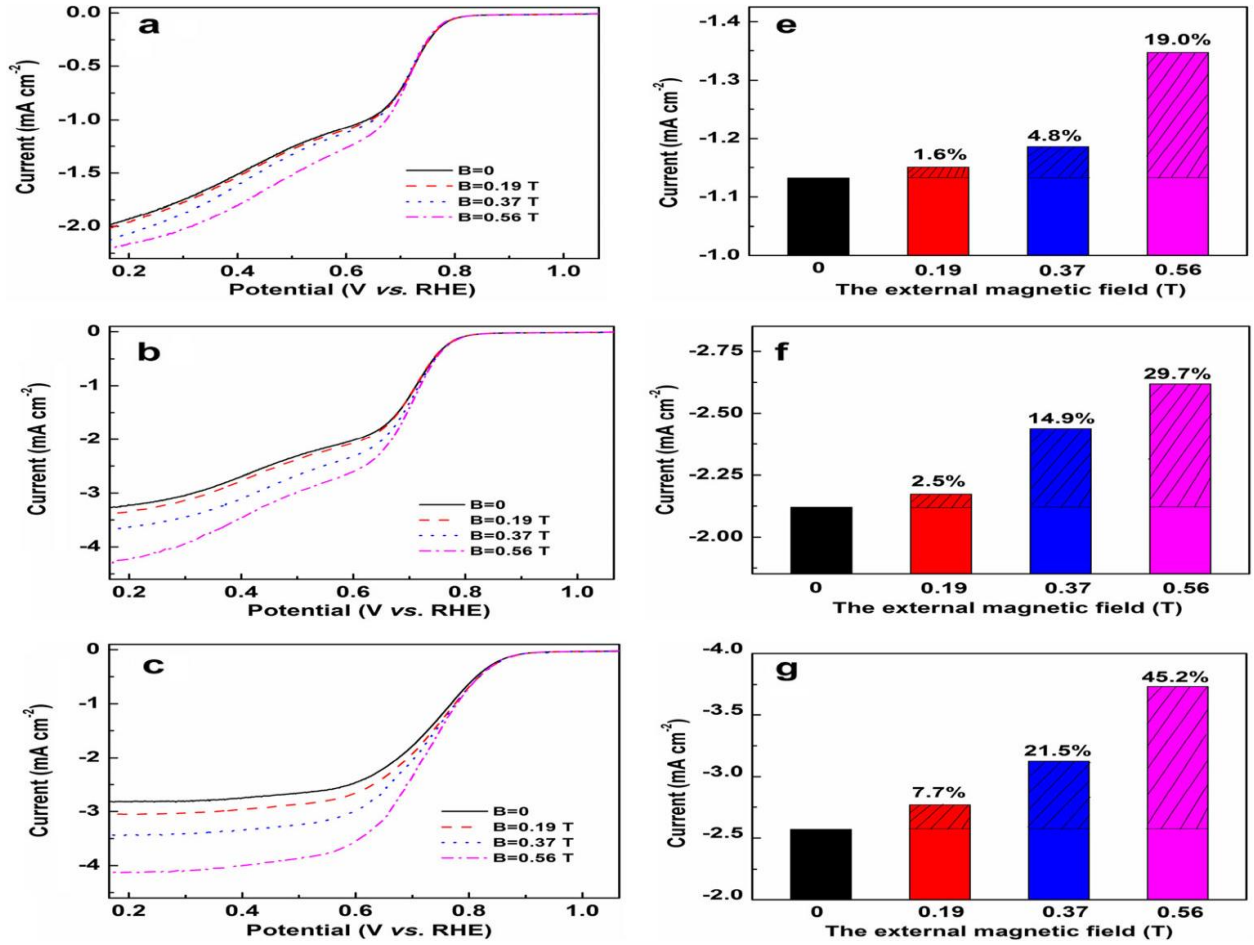

Fig. 4 LSVof Fe3O4 (a), γ- Fe2O3 (b), and Fe-N-C (c) in O2- saturated 0.1 mol L−1 KOH electrolyte at a scan rate of 5 mV s−1 and rotation rate of 1600 rpm under the different external magnetic fields and the corresponding increased range of the ORR current at −0.4 V vs. Ag/AgCl of Fe3O4 (e), γ-Fe2O3 (f), and Fe-N-C (g).

when the Fe3O4 polyaniline load density on the cathode electrode in a zinc air fuel cell is high at 7.11 mg cm−2, the tiny internal magnetic field can also inhibit oxygen transfer because of the interactions between the different magnetic poles .

The result implies that the influence of the tiny internal magnetic field on the catalytic performance for a cathode catalyst is a balance of these opposing factors. In this work, the three catalysts have different saturation magnetizations. When the strength of the applied external magnetic field is larger than the saturation magnetization of Fe-N-C, Fe-N-C is fully magnetically saturated, implying all the tiny magnetic poles in Fe-N-C point to the same direction as the external magnetic field(in fig 5a).

However, for Fe3O4 and γ-Fe2O3, due to their high saturation magnetization, the strength of the applied external magnetic field is lower than their saturation magnetization (as illustrated in Fig. 5b), and then, there are some tiny magnets in Fe3O4 and γ-Fe2O3 samples, whose magnetic pole directions are different from that of the external magnetic field.

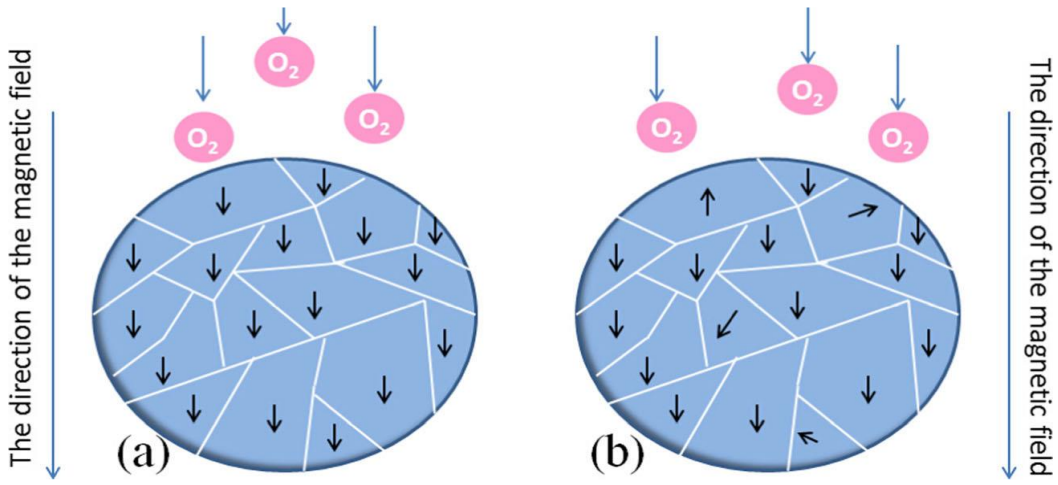

Fig. 5 Influence of the internal tiny magnetic field on O2 transfer under the external magnetic field

The effect of the direction of the external magnetic field was also studied, which was controlled by changing the input current. The obtained results are shown in Fig. 6, which show that the directions of the external magnetic field do not have any effect on the ORR current, because of the paramagnetic property of the oxygen moleculars.

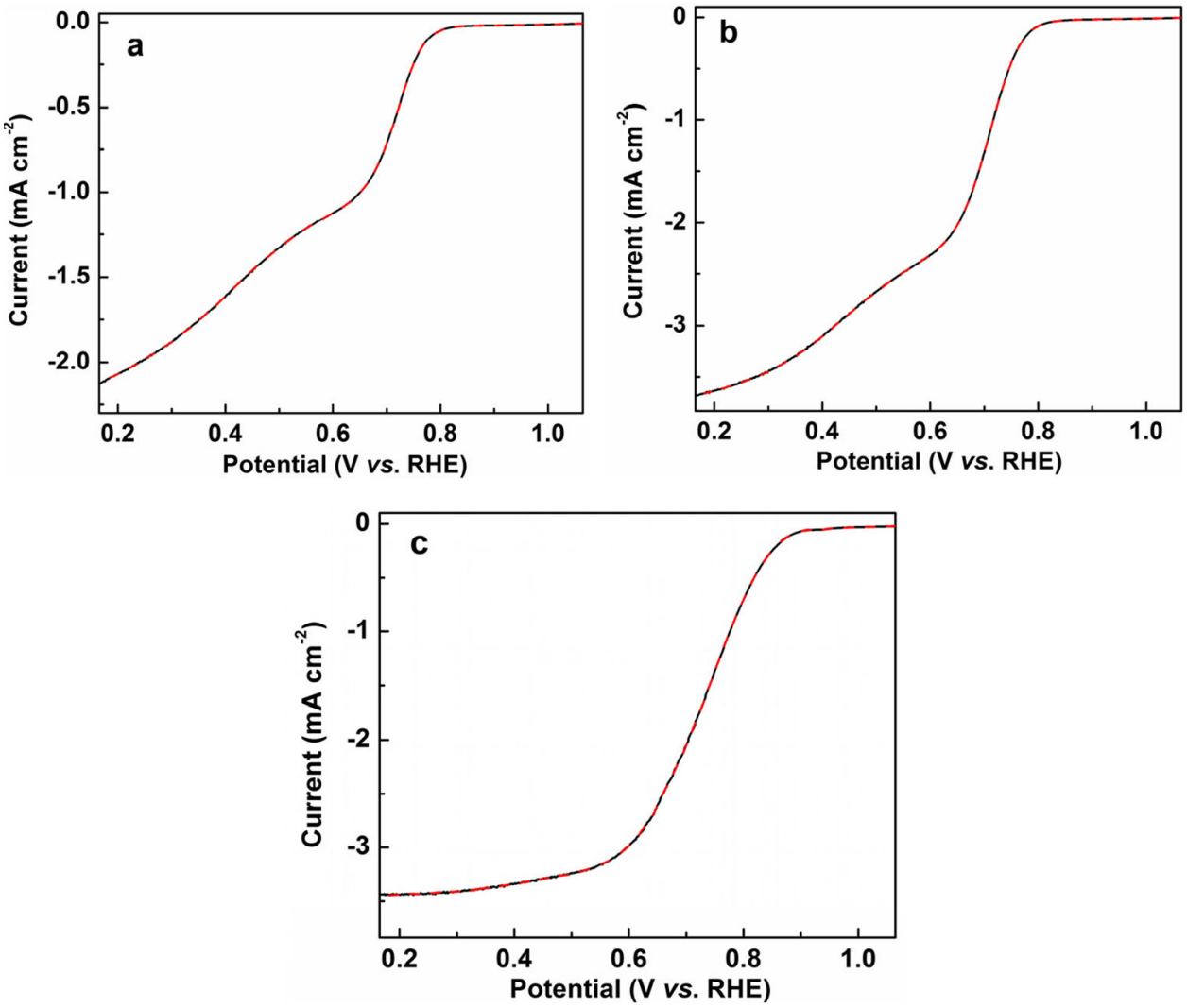

Fig. 6 LSVs of Fe3O4 (a), γ-Fe2O3 (b), and Fe-N-C (c) in O2- saturated 0.1 mol L−1 KOH electrolyte at a scan rate of 5 mV s−1 and rotation rate of 1600 rpm under the external magnetic field (B = 0.37 T) with the opposite direction; black line the direction of the external magnetic field is the same as that used for the previous LSVs in Fig.3; red line the direction of the external magnetic field is opposite to that of the black line

Conclusion:

the ferromagnetic catalysts (including Fe_3O_4, γ-Fe_2O_3, and Fe-N-C) for ORR were studied under the external magnetic fields. It was found that the magnetic force generated by the external magnetic field can facilitate the oxygen transfer, leading to the enhancement of the ORR current on the cathode; moreover, the ORR current on the cathode increases with the strength of the external magnetic field. The internal tiny magnetic field in the ferromagnetic catalysts would lessen the oxygen transfer when the applied external magnetic field is lower than the saturation magnetization of the ferromagnetic catalysts. It was also found that the direction of the external magnetic field does not affect the O_2 transfer due to the paramagnetic property of the oxygen moleculars. The use of external magnets provides a new measure to improve the ORR performance for fuel cells.